

## High- $T_c$ superconducting quantum interference device observation of heat-affected zone in a spot-welded Fe–Cr–Ni system

Yoshimi Watanabe,<sup>a)</sup> S. H. Kang,<sup>b)</sup> J. W. Chan, and J. W. Morris, Jr.

*Center for Advanced Materials, Lawrence Berkeley National Laboratory and Department of Materials Science and Engineering, University of California, Berkeley, California 94720*

John Clarke

*Department of Physics, University of California, Berkeley and Materials Science Division, Lawrence Berkeley National Laboratory, Berkeley, California 94720*

(Received 2 January 2003; accepted 10 June 2003)

A study was carried out to observe a heat-affected zone (HAZ) in a deformed Fe–Cr–Ni system containing  $\alpha'$  martensite using high- $T_c$  superconducting quantum interference device (SQUID) microscopy. Microstructure and remanent magnetization images were studied by an optical microscope and a SQUID microscope, respectively. The HAZ, in which only the face-centered-cubic austenite phase exists, could be visualized by the SQUID microscope. It was also found that the SQUID images were consistent with the results from the microstructural analysis. It was concluded that a simple SQUID measurement may serve as an effective method for a nondestructive evaluation of ferromagnetic steel phases by correlating remanent magnetization images to microstructural characteristics. © 2003 American Institute of Physics.

[DOI: 10.1063/1.1599039]

Spot welding is performed through a resistance welding process in which the components to be welded are clamped between two electrodes supplying heat current. It is known that a weld fusion zone and a heat-affected zone (HAZ), which experience high temperature followed by rapid cooling to room temperature, exhibit very different microstructures, compared with those of base materials.<sup>1</sup> The microstructure of a HAZ is influenced by many factors such as chemical composition, welding condition, and peak temperature. For the analysis of the HAZ microstructure, optical microscope (OM), electron microscope, and x-ray diffraction techniques have been used. In the case of steel, however, their application is limited, since it is difficult to perform a quantitative analysis of HAZ where numerous steel phases such as body-centered-tetragonal martensite ( $\alpha'$ ), hexagonal closed-packed martensite ( $\epsilon$ ), bainite, ferrite ( $\alpha$ ), austenite ( $\gamma$ ), and carbides may coexist.<sup>2</sup>

It is well known that deformation of Fe-18 wt% Cr 9 wt% Ni (stainless steel) introduces an  $\alpha'$  martensite phase within its parent  $\gamma$  austenite phase.<sup>3</sup> This  $\alpha'$  martensite phase can transform into a  $\gamma$  phase (known as the  $\alpha'$  to  $\gamma$  reverse martensitic transformation) when the alloy is heated beyond about 500 °C.<sup>4,5</sup> Since this reverse martensitic transformation is accompanied by a ferromagnetic ( $\alpha'$  phase) to paramagnetic ( $\gamma$  phase) transition, remanent magnetization also changes by this transformation. Accordingly, the remanent magnetization around the HAZ in the deformed stainless steel is expected to change as well. A recent study has shown that the magnetic gradient in a deformed and inhomogeneously heat-treated 304-type stainless steel could be visual-

ized by a superconducting quantum interference device (SQUID) microscope.<sup>5</sup> In SQUID microscopy, a specimen is scanned in close proximity to the SQUID microscope to produce a two-dimensional (2D) magnetic field image.<sup>6–8</sup> In this way, the SQUID microscope can serve as a useful nondestructive evaluation (NDE) tool by precisely measuring the local magnetic field variation that can be related to the characteristics of ferromagnetic materials. Therefore, it is expected that the HAZ in the deformed stainless steel with an  $\alpha'$  martensite phase can be visualized by SQUID microscopy through the difference in remanent magnetization.

In this study, a deformed stainless steel with an  $\alpha'$  martensite phase was spot welded to a copper wire. The welded surfaces and the cross-sectional planes were examined using an OM. A SQUID microscope observation was then carried out on the welded surfaces to produce the 2D remanent magnetization images.

The material used in this study was a commercial grade AISI 304 stainless-steel bar with a cross section of 12.7 mm×6.4 mm. The chemical composition (in wt %) of this stainless steel was: Cr 18.46, Ni 9.04, C 0.033, Mn 1.86, Mo 0.28, Co 0.10, Cu 0.41, P 0.028, Si 0.32, S 0.019, Ti <0.005, V 0.05, and Fe bal. After austenitization at 1050 °C for 2 h, the specimens were rolled down to a rolling ratio of 70% to introduce an  $\alpha'$  martensite phase. The volume fraction of  $\alpha'$  martensite phase was determined to be about 7% by an x-ray diffraction analysis. The diameter of the spot-welded copper wire was 0.5 mm. Heat input powers applied to specimens A and B were 100 W s and 200 W s, respectively.

The specimens were mounted in Transoptic™ powder for the OM and SQUID microscope observation. Since the penetration depth of the SQUID microscope is known to be large while the thickness of the specimens was relatively thin, there was a possibility that the SQUID image includes

<sup>a)</sup>Permanent address: Department of Functional Machinery and Mechanics, Shinshu University, 3-15-1, Tokida, Ueda 386-8567, Japan; electronic mail: yoshimi@gipc.shinshu-u.ac.jp

<sup>b)</sup>Present address: IC Device Technology, Agere Systems, Allentown, PA.



FIG. 1. Microstructure of the welded surface of specimen B, which was welded with a copper wire under the heat input power of 200 W s.

the information from the opposite surface. Therefore, the opposite surface of the SQUID observation specimen was polished carefully before the mounting. The SQUID microscope used in this study is similar in design to other SQUID microscopes.<sup>5–8</sup> The welded specimens were first demagnetized and then subsequently magnetized in fields up to 50 mT, and the vertical component of the remanent magnetization was measured by rastering the specimen over the SQUID using a 2D translation stage with a scanning range of 50 mm. Details of the SQUID microscope are documented elsewhere.<sup>6–8</sup>

The HAZ microstructure was also observed by OM. To observe the HAZ in the stainless steel, a magnetic etching technique<sup>9</sup> was used. Since the unaffected  $\alpha'$  phase and heat-affected  $\gamma$  phase are ferromagnetic and paramagnetic, respectively, this technique revealed only the unaffected ferromagnetic  $\alpha'$  phase.

Figure 1 shows OM microstructure of the welded surfaces of specimen B. It is evident from Fig. 1 that there exists a ferromagnetic  $\alpha'$  martensite phase in the deformed stainless steel. In contrast, only a paramagnetic  $\gamma$  austenite phase is observed near the copper wire, i.e., around the welding point. The starting and finishing temperatures of the reverse martensitic transformation are 450 °C and 650 °C, respectively.<sup>5</sup> This reverse transformation is completed quickly. For example, more than 80% of the reverse transformation occurs within 15 min when the specimen is heated at 670 °C.<sup>4</sup> Therefore, the phenomena shown in Fig. 1 can be explained by the fact that the ferromagnetic  $\alpha'$  martensite phase transformed into the paramagnetic austenite  $\gamma$  phase by the heat generated by the spot welding, while the martensite was exposed to the high temperature only for a short period. In addition, a clear boundary is found between the  $\alpha'$  martensite phase region and the austenite phase region. Since within the range of the starting temperature of the reverse martensitic transformation to the finishing temperature the amount of the martensite phase decreases with increasing temperature, it can be concluded that the temperature gradient around the boundary is steep. This  $\alpha'$  martensite phase free region is the HAZ formed by the spot welding.

Although the OM microstructure of the specimen A is not presented here, a larger austenite phase region (i.e., HAZ) was found for the specimen B. It is known that various welding parameters affect the size of HAZ.<sup>10</sup> The amount of

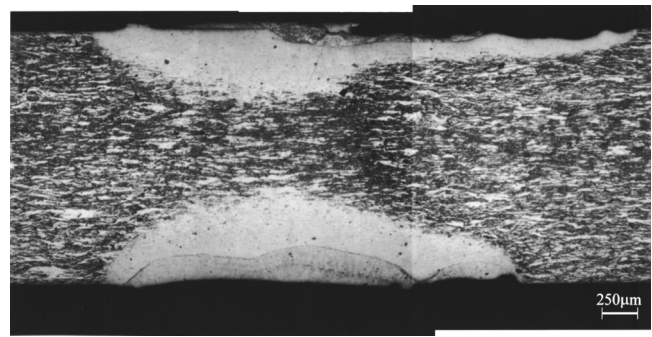


FIG. 2. Cross-sectional view of HAZ in specimen B.

current has greatest influence upon the amount of heat generated.<sup>1</sup> In this study, a larger HAZ was found for specimen B that was welded under a larger heat input power (a larger heat generation during the welding).

In order to investigate the microstructural features around the welding point, cross sections of specimen B were characterized as shown in Fig. 2. The upper and lower surfaces in Fig. 2 correspond to the welding and opposite surfaces, respectively. Note that the dome-shaped HAZ was found at the opposite side of the welding point as well as under the welding point. Again, the size of HAZ increased

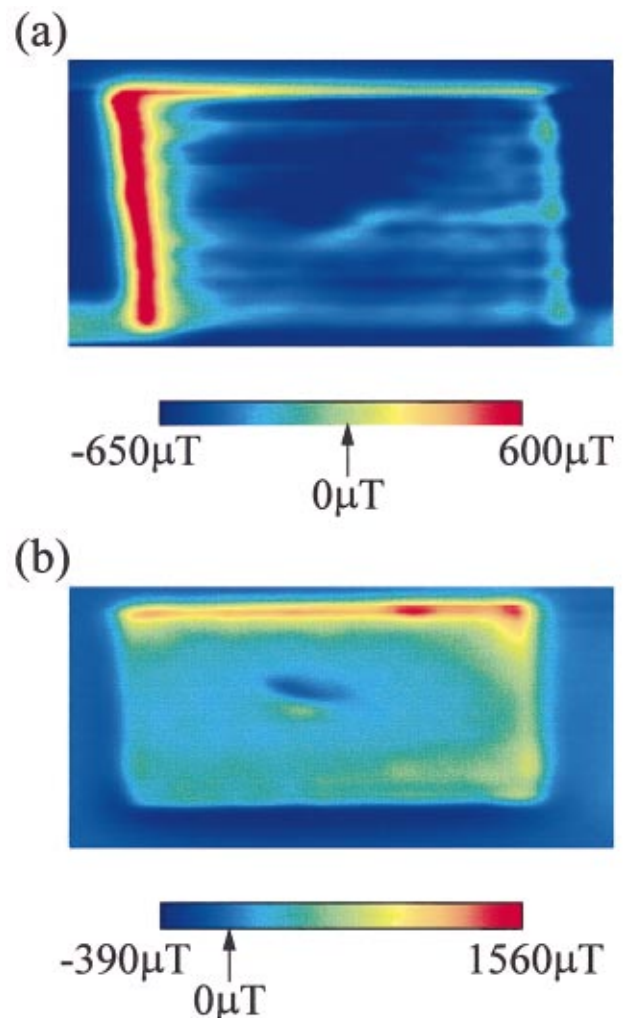


FIG. 3. (Color) The magnetic field images from specimens (a) A and (b) B, respectively.

with increasing the heat input power. In this way, the HAZ where the reverse martensitic transformation takes place can be visualized through the phase difference by the magnetic etching.<sup>9</sup>

Figures 3(a) and 3(b) show the magnetic field images of specimens A and B, respectively, obtained by the SQUID microscope. It must be noted here that a smaller remanent magnetization can be seen at the center region of each specimen at which the HAZ was formed. This is because the phase transformation from the ferromagnetic  $\alpha'$  martensite to the paramagnetic  $\gamma$  austenite occurred at the HAZ. Moreover, a larger remanent magnetization difference was observed for specimen B that was welded under more aggressive conditions. The SQUID images were, thus, in good agreement with the results from the microstructural analysis, suggesting that SQUID microscopy can become a valuable technique that evaluates the reverse martensitic transformation. This microscope may have potential applications not only in detecting phase transformation but also in examining macroscopic defects structures of the materials, such as HAZ.

It should be noted that the SQUID images obtained from the sample edges and corners reflect a geometrical effect rather than a microstructural effect. In each specimen, a large peak was observed at one end of the image. This is due to a so-called edge effect;<sup>8</sup> the corner and edges have a higher remanent magnetization than the center of the specimen. Thus, our results do not contradict the results reported elsewhere.<sup>8</sup>

In summary, a deformed Fe–Cr–Ni steel with the 7 vol%  $\alpha'$  martensite phase was spot welded to a copper wire and characterized using SQUID microscopy. It was found

that the HAZ of the deformed steel, in which only the austenite phase exists, could be identified by the SQUID microscope. While submicron-scaled phenomena in HAZ<sup>11</sup> are still difficult to characterize, a simple SQUID measurement may become an effective method for the NDE of ferromagnetic steel phases by correlating remanent magnetization images to microstructural characteristics.

One of the authors (Y.W.) gratefully acknowledges the financial support from Grant-in-Aid for COE Research (No. 10CE2003) and 21st COE Research by the Ministry of Education, Culture, Sports, Science, and Technology, Japan. The work done at LBNL was supported by the Director, Office of Energy Research, Office of Basic Energy Sciences, U. S. Department of Energy, under Contract No. DE-AC03-76SF00098.

<sup>1</sup>J. S. Campbell, *Principles of Manufacturing Materials and Processes* (McGraw–Hill, New York, 1961), Chap. 17, pp. 375–416.

<sup>2</sup>S. J. Kwon, S. J. Oh, J. H. Kim, S. Kim, and S. Lee, *Scr. Mater.* **40**, 131 (1999).

<sup>3</sup>P. L. Mangonon, Jr. and G. Thomas, *Metall. Trans.* **1**, 1587 (1970).

<sup>4</sup>M. A. M. Bourke, J. G. Maldonado, D. Masters, K. Meggers, and H. G. Priesmeyer, *Mater. Sci. Eng., A* **221**, 1 (1996).

<sup>5</sup>Y. Watanabe, S. H. Kang, J. W. Chan, J. W. Morris, Jr., T. J. Shaw, and J. Clarke, *J. Appl. Phys.* **89**, 1977 (2001).

<sup>6</sup>T. S. Lee, E. Dantsker, and J. Clarke, *Rev. Sci. Instrum.* **67**, 4208 (1996).

<sup>7</sup>T. J. Shaw, K. Schlenga, R. McDermott, J. Clarke, J. W. Chan, S. H. Kang, and J. W. Morris, Jr., *IEEE Trans. Appl. Supercond.* **9**, 4107 (1999).

<sup>8</sup>T. J. Shaw, J. W. Chan, S. H. Kang, R. McDermott, J. W. Morris, Jr., and J. Clarke, *Acta Mater.* **48**, 2655 (2000).

<sup>9</sup>Z. Mei and J. W. Morris, Jr., *Metall. Trans. A* **21A**, 3137 (1990).

<sup>10</sup>C. S. Lee, R. S. Chandel, and H. P. Seow, *Mater. Manuf. Processes* **15**, 649 (2000).

<sup>11</sup>S. Heino, E. M. Knutson-Wedel, and B. Karlsson, *Mater. Sci. Technol.* **15**, 101 (1999).